Does Glutamine Methylation Affect the Intrinsic Conformation of the Universally Conserved GGQ Motif in Ribosomal Release Factors?†

Martin Andér and Johan Åqvist*

Department of Cell and Molecular Biology, Uppsala University, Biomedical Center, Box 596, SE-751 24 Uppsala, Sweden

Received January 26, 2009; Revised Manuscript Received March 2, 2009

ABSTRACT: The GGQ motif is the only universally conserved feature of ribosomal class 1 release factors. Mutational experiments and structural studies have suggested that the glutamine residue of the GGQ motif (Q185 in human eRF1 numbering) is critical for catalysis of the termination reaction on the ribosome. Furthermore, it has been established that Q185 is Nε methylated in prokaryotes as well as eukaryotes, and that methylation significantly enhances the catalytic activity. It is, however, not known whether this methylation affects the intrinsic structure of the free release factor, which could be important for its interaction with the ribosome. In this work, we report molecular dynamics simulations, starting from 25 different NMR structures of human eRF1, in addressing this problem. The results show that there is no such structural effect on the free release factor caused by the Nε methylation of Q185, suggesting that its role is intimately associated with the ribosome environment.

The stop codons UAA, UAG, and UGA are decoded by class I polypeptide chain release factors (RFs)[1] (*1, 2*). Eukaryotic and bacterial class 1 RFs have very different primary structures and seem to have evolved in a manner independent of each other (*3*). In eukaryotes, mitochondria, and archaea, a single class I polypeptide chain release factor (eRF1, mRF1, and aRF1, respectively) recognizes all stop codons (*3*−*7*), while in bacteria, two different RFs (RF1 and RF2) exist, with partially overlapping stop codon specificity (*8*). RFs preferentially bind to cognate stop codons compared to noncognate codons by a factor of 10^3−10^6, without the help of a proofreading mechanism (*9*), and the mechanism by which RFs recognize mRNA stop codons long remained a mystery. Recent papers by Laurberg et al. (*10*), Weixlbaumer et al. (*11*), and Korostelev et al. (*12*) report the first crystallographic structures that show RF−stop codon interactions in detail.

The only primary sequence feature of the class I polypeptide release factors that is universally conserved across all kingdoms of life is the GGQ motif present in domain 2 of eRF1 and domain 3 of prokaryotic RFs. This motif has been suggested to be directly involved in the mechanism by which, presumably, all RFs catalyze the hydrolysis reaction that releases the nascent peptide from the A-site aa-tRNA in the PTC (*5, 13, 14*). Earlier results from both cryo-electron microscopy and low-resolution X-ray crystallography of RFs bound to the ribsome indicated that the loop containing the GGQ motif is in the immediate vicinity of the PTC (*15*−*17*). These studies further showed that the conformations of RF1 and RF2 bound to the ribosome are similar to their solution structures (*18*) but differ from the corresponding crystal structures of free release factors (*13, 19*).

Computer simulation and docking studies by Trobro and Åqvist (*14*) predicted that the GGQ motif interacts with the ribosome in such a way that the glutamine side chain inserts into the A-site, where it can coordinate a water molecule that hydrolyzes the peptidyl-tRNA ester bond through a mechanism similar to that of the peptidyl transfer reaction (*20*−*22*). The recent medium-resolution (∼3 Å) crystal structrures of RF1 and RF2 complexes with the ribosome confirmed that the glutamine residue indeed inserts in the A-site, making contact with the P-site substrate (*10, 11*). The fact that the relevant parts of domain V of the 23S/28S rRNA constituting the PTC are universally conserved (*23*), as is the GGQ motif, thus strongly suggests that the critical interactions between the RFs and the PTC are also conserved. Mutation of the central glycine in the GGQ motif to alanine has been shown to result in a dramatic loss of activity (*24*), pointing to a key role of the GGQ backbone conformation in catalysis (*10, 11, 14*). On the other hand, mutation of the glutamine residue to alanine has only a minor effect, while its substitutions with Asn or Asp are severe (*25*), suggesting that detailed interactions involving this side chain are important for catalysis.

It is obvious via examination of the structures of the PTC, the medium-resolution crystal structures of the bacterial RF1 and RF2 complexes with ribosome (*10, 11*) (PDB entries 3D5A−3D5D and 2JL5−2JL8, respectively), and the available crystal and NMR structures of free eukaryotic RFs (PDB entries 1DT9 and 2HST) (*13, 26*), that the GGQ-containing loop must undergo some structural rearrangements to reach into the PTC [it should be noted here that the available crystal structures of free bacterial release factors (*19, 27*) have ill-defined electron density for the GGQ loop and are not suitable for such comparisons]. Specifically, for the side chain of Q185 (human eRF1 numbering) to be able to adopt the

† Support from the Swedish Research Council (VR) is gratefully acknowledged.

* To whom correspondence should be addressed. Phone: +46 18 471 41 09. Fax: +46 18 53 69 71. E-mail: aqvist@xray.bmc.uu.se.

[1] Abbreviations: MD, molecular dynamics; rmsd, root-mean-square deviation; RF, release factor; PDB, Protein Data Bank.

10.1021/bi900117r CCC: $40.75
Published on Web 03/05/2009

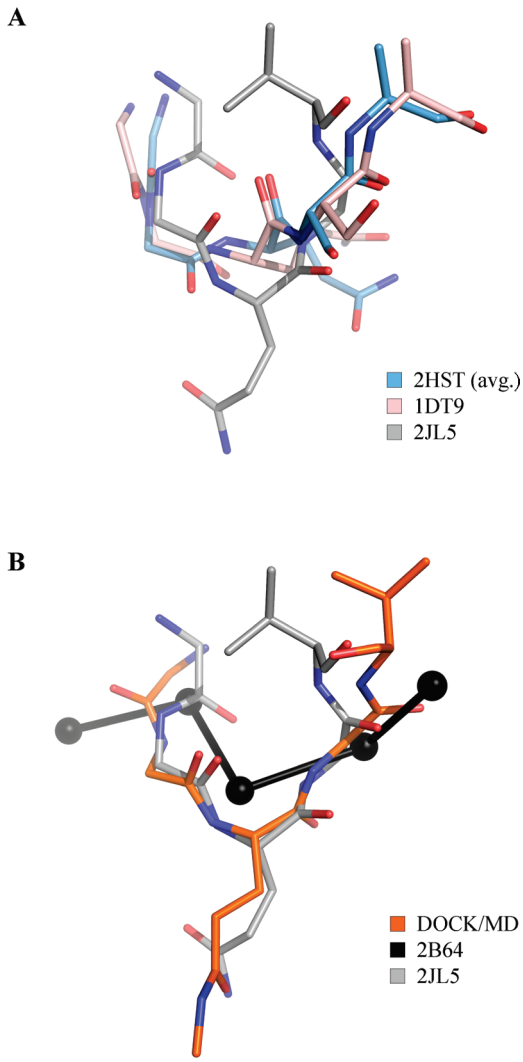

FIGURE 1: Views of residues 183−187 (human eRF1 numbering) from five different published structures of the GGQ loop: (A) crystal structure of free eRF1 (pink) (*13*) and the average structure of 25 NMR models of eRF1 in solution (blue) (*26*) compared to the medium-resolution crystal structure of RF2 bound to the ribosome (gray) (*11*) and (B) the structure predicted using docking and MD/EVB calculations (orange) (*14*) and the Cα trace from the earlier low-resolution crystal structure of the RF2−ribosome complex (black) (*17*) compared to the structure of RF2 bound to the ribosome (gray) (*11*). All structures have been fitted to the structure of RF2 to minimize the backbone rmsd.

conformation it is predicted to have in the PTC during peptide release (pointing away from the rest of the RF toward the nascent peptide attached to the CCA end of the P-site aa-tRNA), it must move away from the rest of the RF (*10, 11*). This is illustrated in Figure 1A which shows the conformations of the residues surrounding Q185 in the free RF structures compared to the ribosome complex. Figure 1B shows the very similar conformations of the GGQ loop generated by automated docking and molecular dynamics (MD) simulation (*14*) and the subsequently published 2JL5 crystal structure (*11*), as well as the significantly differing loop model (Cα trace) from the low-resolution RF−ribosome complex (*17*).

The glutamine residue of the GGQ motif has been shown to be methylated at the Nε position in both prokaryotes and eukaryotes, and this methylation significantly enhances the rate by which the ribosomal machinery catalyzes peptide release both in vitro and in vivo (*28*−*32*). The computer simulations of the termination reaction, which were based on automated docking of a heptapeptide fragment containing the GGQ motif, were conducted both with and without the Gln methylation, and the calculations showed a clear contribution to catalysis from the Nε methylation (*14*). It is thus evident that the Nε methylation of Q185 has a significant effect on catalysis of the termination reaction, but it is not known whether the methylation may have an effect of the intrinsic structural preference of the GGQ loop. This is particularly so because all the published structures of RFs differ from the in vivo situation in having regular, nonmethylated, glutamine residues in the GGQ motif (*10*−*13, 16*−*18, 26, 27*). If, for example, the methylation of Q185 stabilizes a free state conformation of the RF closer to that of the bound state, it is plausible that the cost in free energy due to entropy loss associated with binding to the ribosome would decrease (*33, 34*). It is, thus, conceivable that the role of Gln methylation might be to predispose the loop and/or side chain to a productive conformation in the termination reaction. Conversely, it may be the case that methylation has no effect on the intrinsic conformational preference but provides a key effect only in the ribosome environment. To shed light on this issue, it is therefore of considerable interest to try to study the structural effects of Nε methylation of Q185.

The recently published solution NMR structure of the middle domain of eRF1 provides an excellent starting point for molecular dynamics simulations of the GGQ-containing loop (*26*). This NMR structure (PDB entry 2HST) contains 25 solutions, all of which are relatively similar, except for in the GGQ loop, which seems to possess a significant degree of flexibility. By performing a set of identically initialized MD simulations starting from each of the 25 deposited NMR solutions, with Q185 in both its standard and methylated forms, we can undertake a thorough investigation of the possible structural effects of Nε methylation of Q185.

MATERIALS AND METHODS

To probe the effect of Nε methylation of Q185 on the structure of the GGQ-containing loop, free eRF1 in water solution was studied using extensive MD simulations. All MD simulations were carried out using the software package Q, in combination with the OPLS all-atom force field (*35, 36*). Starting coordinates were obtained from the recently published NMR structures of the middle domain of human eRF1 free in solution (PDB entry 2HST) (*26*). The corresponding initial structures for Q185 Nε methylated eRF1 were obtained by manually replacing the relevant hydrogen atom of Q185 with a methyl group. Replicate simulations were performed for each of the 25 NMR solution structures, yielding a total of 50 simulation systems (nonmethylated and methylated). The MD simulations were performed in a spherical system with a 20 Å radius centered on the Cα atom of G184 (the central glycine residue in the GGQ motif). TIP3P water was used to solvate the systems, using the SCAAS boundary conditions, under which the water molecules near the surface of the sphere are subjected to radial and polarization restraints to mimic the properties of bulk water (*37, 38*). Solute atoms outside the 20 Å simulation sphere were tightly restrained throughout the simulation. Nonbonded interactions across the

simulation sphere boundary were excluded. A 10 Å cutoff radius was used for all nonbonded interactions, along with the local reaction field (LRF) multipole expansion treatment of long-range electrostatic interactions beyond the cutoff (*39*). The reported results herein are from simulations conducted at zero ionic strength, but a complete set of trajectories was also initially calculated with chloride counterions in the solution. However, the two different ionic strengths give virtually identical results, and we considered the 0 M case to be more physiologically relevant than the ~0.3 M case (both yield an rmsd of 0.6 Å for unfitted backbone atoms of residues 183−187 between methylated and nonmethylated total MD average structures and 2.1 and 2.9 Å unfitted rmsds between the nonmethylated MD and average NMR structures, respectively). Prior to production phase MD, equilibration was performed by stepwise heating from 10 to 300 K, accompanied by gradual loosening of heavy atom restraints. For each system, the production phase consisted of 500 ps of unrestrained MD at 300 K, with a time step of 1 fs in conjunction with the SHAKE procedure for all solvent bonds (*40*). Thus, the total simulation time for these systems was 25 ns (2 × 25 × 500 ps). For the sake of comparison, we also calculated two longer trajectories of ~15 ns each for the methylated and nonmethylated case starting from the central NMR structure.

RESULTS

The relatively high flexibility of the GGQ loop is already suggested by the spread of the 25 NMR solutions of eRF1, as shown in Figure 2A, and relaxation and order parameters from the NMR experiments also verify the mobility of this region (*26*). The loop is apparently the most disordered part of the protein structure with relatively few long- and medium-range NOEs and torsional restraints. However, it is not immediately obvious by looking at the NMR structures (Figure 2A) whether the local conformations of the residues surrounding Q185 are significantly different between the different NMR models or whether the flexibility of the loop is limited to rigid-body-like displacement of one or several portions of the loop. Figure 2B shows residues 183−187 of all 25 models in 2HST, fitted to locally minimize the backbone rmsd between each solution structure and the central most representative structure of the NMR family. This figure clearly demonstrates that the local conformation of the residues surrounding Q185 is fairly similar in all 25 solutions in the 2HST structure, arguably similar enough not to be separated by any large free energy barriers, and thus to be thermally accessible at ambient temperatures.

To be able to draw conclusions from comparisons of MD simulations of the highly flexible GGQ loop in its nonmethylated and methylated forms, it must first be asserted that MD simulations of the nonmethylated structure sample physically relevant regions of conformational space. That is, the MD average structure of the nonmethylated GGQ loop should closely resemble the corresponding experimental NMR solution structures for us to be able to use it as a basis for comparison with MD simulations of its methylated counterpart. We considered the most unbiased computational strategy to be to carry out shorter independent simulations starting from each of the 25 NMR solutions, but as a comparison, we also calculated two longer trajectories (each

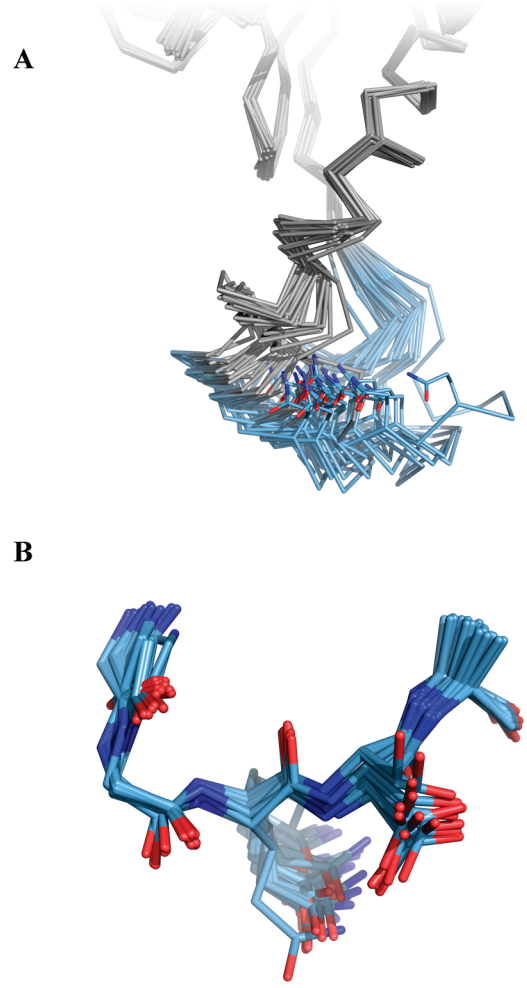

FIGURE 2: Structural variation of the GGQ loop in the 25 NMR solutions from 2HST (*26*). (A) Unfitted conformations of residues 177−188 (colored blue, with Q185 shown in stick representation). (B) Conformations of the residues surrounding Q185, after fitting to minimize the backbone rmsd to the central structure of the NMR family.

~15 ns) for the methylated and nonmethylated Gln starting from the central NMR structure (see below). Figure 3A shows the total 12.5 ns average MD structure of the nonmethylated loop, obtained from the 25 independent simulations, in relation to the average NMR structure. This average structure is calculated without any least-squares fitting to reference coordinates, so that the overall positioning of the GGQ loop relative to the rest of the protein can be directly compared to the NMR results. As one can see from Figure 3A, the agreement between the average NMR and MD structures is generally very good and the unfitted rmsd of all heavy backbone atoms of residues 177−188 is 2.1 Å, while the corresponding heavy atom rmsd including the side chains is 2.3 Å. The main difference between the MD and NMR structures is a displacement of the backbone segment comprising residues 180−182, for which there are no long-range NOE or backbone torsional restraints in the NMR data (*26*). Note that the similar conformations of the total 12.5 ns MD average structure and the average NMR structure are not simply a result of each individual 500 ps MD trajectory sampling the region immediately surrounding its starting (NMR) structure, thereby generating 500 ps subaverages that are very close to their respective initial conformation (see below).

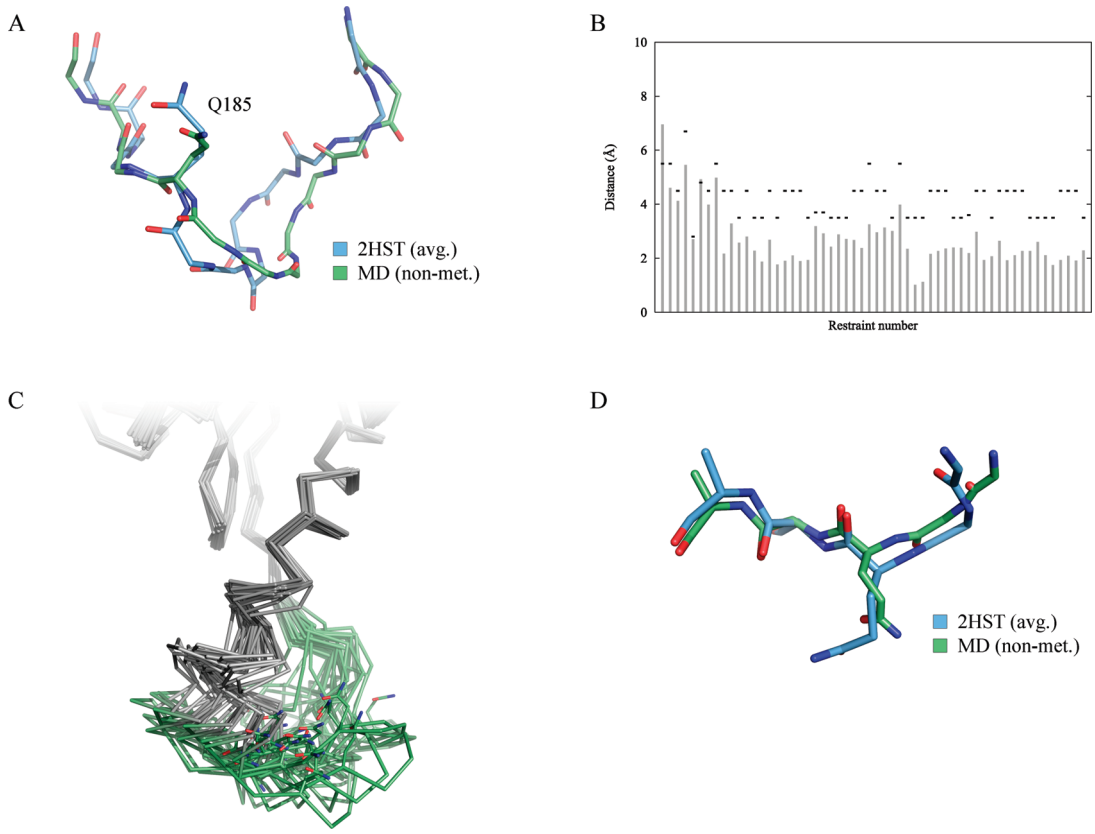

FIGURE 3: (A) Residues 177−188 of the average NMR structure (blue) (*26*) compared to the overall MD average structure (green) of the nonmethylated GGQ loop. (B) NOE distance restraints involving H, Hα, and Hβ atoms in residues 177−188 (black horizontal bars denoting upper limits) compared to distance measurements in the MD average structure (gray vertical bars). (C) Conformational variation among the 25 individual MD average structures of the nonmethylated GGQ loop. (D) Residues 183−187 of the average NMR structure (blue) (*26*) and the overall MD average structure (green) fitted to minimize the backbone rmsd. The bond lengths of the Q185 side chain appear unphysically short in the MD structure due to averaging effects.

The total 12.5 ns average MD structure can also be compared directly to the NMR restraints (i.e., to the raw data rather than to the models derived form it), and Figure 3B shows that the experimental distance restraints are qualitatively satisfied by the MD structure. It could be argued that the fairly short simulation times of 500 ps in combination with a starting conformation obtained from an NMR model would automatically result in an average structure that satisfies the NMR restraints that were used to build the model. Note, however, that in this case the average structure is calculated over 25 different trajectories, with 25 different starting conformations. Even if the average structures obtained from the individual 500 ps trajectories would all satisfy the NMR restraints perfectly because they did not deviate from their respective starting (NMR) conformations (which is not the case; see below), this would not imply that the total average structure would also do so. The one NMR restraint in Figure 3B which is not satisfied by the total MD average structure of the nonmethylated GGQ-containing loop is between the Hβ and H atoms of residues Q185 and K179. This restraint is also violated by 10 of the 25 NMR models themselves, including the central structure.

It is also useful to examine the spread of the 25 individual average MD structures of the nonmethylated loop, and Figure 3C shows these structures in the same view as Figure 2A. It can immediately be seen that the spread of these subaverage structures is similar to that of the NMR models. However, an important property of these MD subaverages is that they do not correlate in general with their starting structures. That is, the similarity of the conformational spread in Figures 2A and 3C does not reflect a situation in which each simulation is trapped around its initial structure. On the contrary, the average unfitted backbone rmsd between structures in Figures 2A and 3C corresponding to the same simulation is 3.8 Å (individual rmsds between the average MD structures and their starting NMR conformation range between 2.5 and 7.0 Å), which is significantly larger than the rmsd between the overall average MD and NMR structures. When examining the results from the two longer simulations (i.e., both nonmethylated and methylated loop) starting from the central NMR structure, one finds that these single trajectories span a much smaller region of the conformational space and that their average structures deviate considerably more from the NMR average (data not shown). This appears to be due to a propensity for ion pair formation between the two arginines at positions 182 and 189 and D175 and E196, respectively. These ion pairs apparently form and break on a rather long time scale so that trajectories where they occur would require much longer simulations for adequate sampling. This illustrates the danger of using single MD trajectories in the analysis that may have become biased by the starting structure and velocities.

We will thus base our conclusions on the 25 shorter independent trajectories of the nonmethylated and methylated GGQ loops as these simulations by all criteria are the most unbiased and are found to sample relevant regions of conformational space. In a highly flexible structure such as the GGQ-containing loop, it is also important to keep in mind

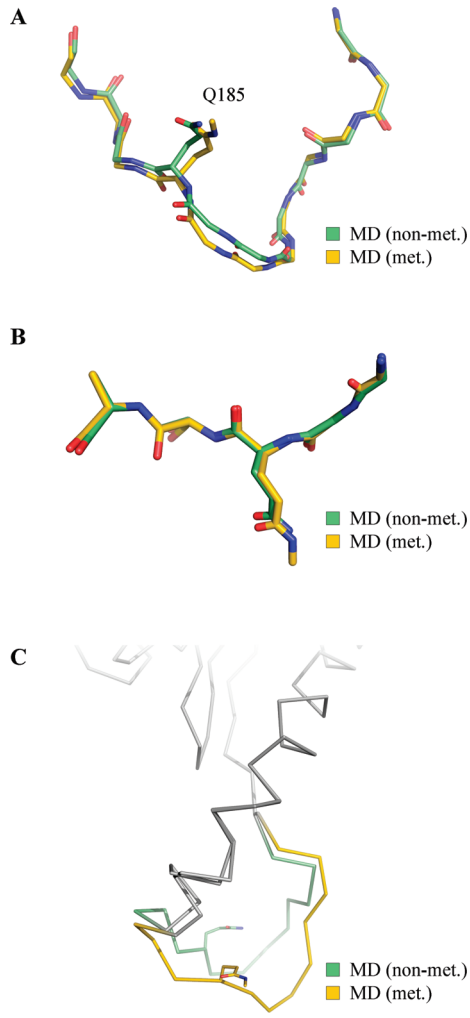

FIGURE 4: Conformations of the GGQ loop in the nonmethylated (green) and methylated (yellow) overall MD average structures: (A) residues 177−188 unfitted and (B) residues 183−187 fitted to minimize the backbone rmsd. (C) View of a nonmethylated and a methylated 500 ps average structure originating from the same starting conformation.

that possible structural changes due to Gln methylation could be either global or local. In the simulations presented here, residues 176−193 are completely free to move relative to the fixed portion of the release factor, outside the simulation sphere, yet the average unfitted MD structure of the nonmethylated loop agrees very well with the corresponding NMR structure as seen above. The local conformation of the nonmethylated GGQ loop in these two structures is compared in Figure 3D, where the backbone atoms of resiudes 183−187 have been least-squares fitted with a resulting rmsd of only 0.85 Å. Clearly, also the local conformation around Gln185 is, on average, virtually identical in the calculated and observed structures.

Turning now to the case with Gln185 methylated, we find that both the global and local conformation of the GGQ loop is completely unaffected by the methylation. The rmsd of all heavy backbone atoms of residues 177−188 between the unfitted nonmethylated and methylated MD average structures is 0.6 Å, and the corresponding heavy atom rmsd including the side chains is 0.7 Å (Figure 4A). As for the local conformation, fitting of the two overall average MD structures with respect to the backbone of residues 183−187 results in an almost perfect overlap with an rmsd of 0.19 Å (Figure 4B). Again, as with the comparison between the total MD average structure of the nonmethylated loop and the average NMR structure, it is important to note that the striking structural similarity is not a result of each 500 ps simulation of the methylated GGQ-containing loop resulting in the same average structure as its nonmethylated counterpart originating from the same starting (NMR) conformation. Rather, the average structures of individual 500 ps nonmethylated and methylated simulations originating from the same starting conformation differ by as much as 6.9 Å in terms of the backbone rmsd of residues 183−187 (Figure 4C). On average, the rmsd between the backbone atoms of residues 183−187 of two corresponding nonmethylated and methylated 500 ps average structures is as large (3.8 Å) as the average rmsd between the different starting conformations and the central model in the NMR family (3.9 Å). This further illustrates the highly flexible nature of the GGQ-containing loop and underlines the significance of the very high degree of similarity between the nonmethylated and methylated 12.5 ns total average structures.

Ramachandran plots of residues 183−187 of the 25 starting (NMR) conformations and of four evenly spaced snapshots from each of the 25 MD trajectories of the nonmethylated and methylated loop are presented in Figure 5. Figure 5A shows that the backbone of G183 and G184 exists in a few different conformations in the NMR family

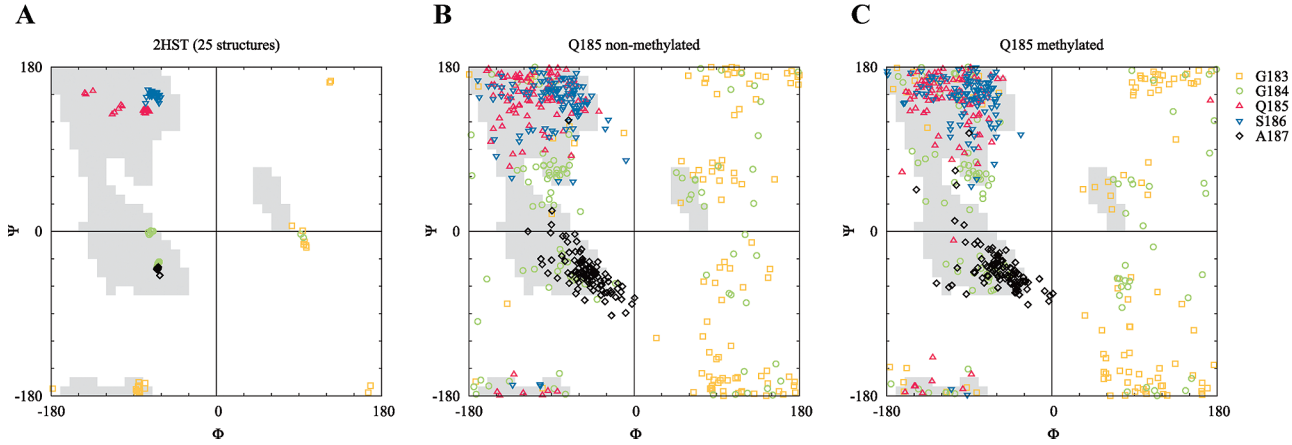

FIGURE 5: (A) Ramachandran plots for residues 183−187 of the 25 NMR solutions in 2HST (*26*), (B) 100 snapshots from the 25 MD simulations of the nonmethylated GGQ loop, and (C) 100 snapshots from the simulations of the methylated loop. Data for the two glycine residues are shown in pale colors for the sake of clarity.

of structures, while Q185, S186, and A187 are rather restricted in $\phi-\psi$ space. Panels B and C of Figure 5 demonstrate that while the backbone of Q185, S186, and A187 is fairly flexible during MD simulation, the three residues stay within the allowed regions and the fluctuations are essentially centered around their average NMR conformations. As expected, the backbone conformations of G183 and G184 fluctuate dramatically during the MD simulations, with data points in every quadrant of the Ramachandran plots (Figure 5B,C). In this respect, too, the nonmethylated and methylated simulations yield similar results and are not distinct from each other (Figure 5B,C).

CONCLUSIONS

The glutamine residue of the universally conserved GGQ motif of class 1 ribosomal release factors has been found to be methylated at the Nε position in all kingdoms of life (*28*−*32*). In this work, we have addressed the question of whether this methylation has an intrinsic effect on the conformational preference of the GGQ loop, which could be important for its interaction with the ribosome. By carrying out a total of 25 ns of MD simulations of the relevant part of domain 2 of eRF1 that contains the GGQ loop, utilizing 25 different NMR models as initial structures, we explored the conformational effects of methylating Q185. The MD simulations show very convincing agreement with the NMR results for the nonmethylated loop and suggest that there is no discernible conformational difference between the methylated and nonmethylated cases. We can thus conclude that while the MD trajectories for the two loops explore large regions of conformational space, they both converge to the same average structure, indicating that the Nε methylation of Q185 does not have a structural effect on the free release factor.

REFERENCES

1. Capecchi, M. R. (1967) Polypeptide Chain Termination in Vitro: Isolation of a Release Factor. *Proc. Natl. Acad. Sci. U.S.A. 58*, 1144–1151.
2. Petry, S., Weixlbaumer, A., and Ramakrishnan, V. (2008) The termination of translation. *Curr. Opin. Struct. Biol. 18*, 70–77.
3. Frolova, L., Legoff, X., Rasmussen, H. H., Cheperegin, S., Drugeon, G., Kress, M., Arman, I., Haenni, A. L., Celis, J. E., Philippe, M., Justesen, J., and Kisselev, L. (1994) A Highly Conserved Eukaryotic Protein Family Possessing Properties of Polypeptide-Chain Release Factor. *Nature 372*, 701–703.
4. Konecki, D. S., Aune, K. C., Tate, W., and Caskey, C. T. (1977) Characterization of Reticulocyte Release Factor. *J. Biol. Chem. 252*, 4514–4520.
5. Frolova, L. Y., Tsivkovskii, R. Y., Sivolobova, G. F., Oparina, N. Y., Serpinsky, O. I., Blinov, V. M., Tatkov, S. I., and Kisselev, L. L. (1999) Mutations in the highly conserved GGQ motif of class 1 polypeptide release factors abolish ability of human eRF1 to trigger peptidyl-tRNA hydrolysis. *RNA 5*, 1014–1020.
6. Bult, C. J., White, O., Olsen, G. J., Zhou, L. X., Fleischmann, R. D., Sutton, G. G., Blake, J. A., FitzGerald, L. M., Clayton, R. A., Gocayne, J. D., Kerlavage, A. R., Dougherty, B. A., Tomb, J. F., Adams, M. D., Reich, C. I., Overbeek, R., Kirkness, E. F., Weinstock, K. G., Merrick, J. M., Glodek, A., Scott, J. L., Geoghagen, N. S. M., Weidman, J. F., Fuhrmann, J. L., Nguyen, D., Utterback, T. R., Kelley, J. M., Peterson, J. D., Sadow, P. W., Hanna, M. C., Cotton, M. D., Roberts, K. M., Hurst, M. A., Kaine, B. P., Borodovsky, M., Klenk, H. P., Fraser, C. M., Smith, H. O., Woese, C. R., and Venter, J. C. (1996) Complete genome sequence of the methanogenic archaeon, *Methanococcus jannaschii*. *Science 273*, 1058–1073.
7. Klenk, H. P., Clayton, R. A., Tomb, J. F., White, O., Nelson, K. E., Ketchum, K. A., Dodson, R. J., Gwinn, M., Hickey, E. K., Peterson, J. D., Richardson, D. L., Kerlavage, A. R., Graham, D. E., Kyrpides, N. C., Fleischmann, R. D., Quackenbush, J., Lee, N. H., Sutton, G. G., Gill, S., Kirkness, E. F., Dougherty, B. A., McKenney, K., Adams, M. D., Loftus, B., Peterson, S., Reich, C. I., McNeil, L. K., Badger, J. H., Glodek, A., Zhou, L. X., Overbeek, R., Gocayne, J. D., Weidman, J. F., McDonald, L., Utterback, T., Cotton, M. D., Spriggs, T., Artiach, P., Kaine, B. P., Sykes, S. M., Sadow, P. W., DAndrea, K. P., Bowman, C., Fujii, C., Garland, S. A., Mason, T. M., Olsen, G. J., Fraser, C. M., Smith, H. O., Woese, C. R., and Venter, J. C. (1997) The complete genome sequence of the hyperthermophilic, sulphate-reducing archaeon *Archaeoglobus fulgidus*. *Nature 390*, 364–370.
8. Scolnick, E., Tompkins, R., Caskey, T., and Nirenberg, M. (1968) Release Factors Differing in Specificity for Terminator Codons. *Proc. Natl. Acad. Sci. U.S.A. 61*, 768–774.
9. Freistroffer, D. V., Kwiatkowski, M., Buckingham, R. H., and Ehrenberg, M. (2000) The accuracy of codon recognition by polypeptide release factors. *Proc. Natl. Acad. Sci. U.S.A. 97*, 2046–2051.
10. Laurberg, M., Asahara, H., Korostelev, A., Zhu, J. Y., Trakhanov, S., and Noller, H. F. (2008) Structural basis for translation termination on the 70S ribosome. *Nature 454*, 852–857.
11. Weixlbaumer, A., Jin, H., Neubauer, C., Voorhees, R. M., Petry, S., Kelley, A. C., and Ramakrishnan, V. (2008) Insights into Translational Termination from the Structure of RF2 Bound to the Ribosome. *Science 322*, 953–956.
12. Korostelev, A., Asahara, H., Lancaster, L., Laurberg, M., Hirschi, A., Zhua, J. Y., Trakhanov, S., Scott, W. G., and Noller, H. F. (2008) Crystal structure of a translation termination complex formed with release factor RF2. *Proc. Natl. Acad. Sci. U.S.A. 105*, 19684–19689.
13. Song, H. W., Mugnier, P., Das, A. K., Webb, H. M., Evans, D. R., Tuite, M. F., Hemmings, B. A., and Barford, D. (2000) The crystal structure of human eukaryotic release factor eRF1: Mechanism of stop codon recognition and peptidyl-tRNA hydrolysis. *Cell 100*, 311–321.
14. Trobro, S., and Åqvist, J. (2007) A model for how ribosomal release factors induce peptidyl-tRNA cleavage in termination of protein synthesis. *Mol. Cell 27*, 758–766.
15. Rawat, U. B. S., Zavialov, A. V., Sengupta, J., Valle, M., Grassucci, R. A., Linde, J., Vestergaard, B., Ehrenberg, M., and Frank, J. (2003) A cryo-electron microscopic study of ribosome-bound termination factor RF2. *Nature 421*, 87–90.
16. Klaholz, B. P., Pape, T., Zavialov, A. V., Myasnikov, A. G., Orlova, E. V., Vestergaard, B., Ehrenberg, M., and van Heel, M. (2003) Structure of the *Escherichia coli* ribosomal termination complex with release factor 2. *Nature 421*, 90–94.
17. Petry, S., Brodersen, D. E., Murphy, F. V., Dunham, C. M., Selmer, M., Tarry, M. J., Kelley, A. C., and Ramakrishnan, V. (2005) Crystal structures of the ribosome in complex with release factors RF1 and RF2 bound to a cognate stop codon. *Cell 123*, 1255–1266.
18. Vestergaard, B., Sanyal, S., Roessle, M., Mora, L., Buckingham, R. H., Kastrup, J. S., Gajhede, M., Svergun, D. I., and Ehrenberg, M. (2005) The SAXS solution structure of RF1 differs from its crystal structure and is similar to its ribosome bound cryo-EM structure. *Mol. Cell 20*, 929–938.
19. Vestergaard, B., Van, L. B., Andersen, G. R., Nyborg, J., Buckingham, R. H., and Kjeldgaard, M. (2001) Bacterial polypeptide release factor RF2 is structurally distinct from eukaryotic eRF1. *Mol. Cell 8*, 1375–1382.
20. Weinger, J. S., Parnell, K. M., Dorner, S., Green, R., and Strobel, S. A. (2004) Substrate-assisted catalysis of peptide bond formation by the ribosome. *Nat. Struct. Mol. Biol. 11*, 1101–1106.
21. Trobro, S., and Åqvist, J. (2005) Mechanism of peptide bond synthesis on the ribosome. *Proc. Natl. Acad. Sci. U.S.A. 102*, 12395–12400.
22. Rodnina, M. V., Beringer, M., and Wintermeyer, W. (2007) How ribosomes make peptide bonds. *Trends Biochem. Sci. 32*, 20–26.
23. Cannone, J. J., Subramanian, S., Schnare, M. N., Collett, J. R., D'Souza, L. M., Du, Y. S., Feng, B., Lin, N., Madabusi, L. V., Muller, K. M., Pande, N., Shang, Z. D., Yu, N., and Gutell, R. R. (2002) The Comparative RNA Web (CRW) Site: An online database of comparative sequence and structure information for ribosomal, intron, and other RNAs. *BMC Bioinf. 3*, 2.

24. Zavialov, A. V., Mora, L., Buckingham, R. H., and Ehrenberg, M. (2002) Release of peptide promoted by the GGQ motif of class 1 release factors regulates the GTPase activity of RF3. *Mol. Cell 10*, 789–798.
25. Shaw, J. J., and Green, R. (2007) Two distinct components of release factor function uncovered by nucleophile partitioning analysis. *Mol. Cell 28*, 458–467.
26. Ivanova, E. V., Kolosov, P. M., Birdsall, B., Kelly, G., Pastore, A., Kisselev, L. L., and Polshakov, V. I. (2007) Eukaryotic class I translation termination factor eRF1: The NMR structure and dynamics of the middle domain involved in triggering ribosome-dependent peptidyl-tRNA hydrolysis. *FEBS J. 274*, 4223–4237.
27. Zoldak, G., Redecke, L., Svergun, D. I., Konarev, P. V., Voertler, C. S., Dobbek, H., Sedlak, E., and Sprinzl, M. (2007) Release Factors 2 from *Escherichia coli* and *Thermus thermophilus*: Structural, spectroscopic and microcalorimetric studies. *Nucleic Acids Res. 35*, 1343–1353.
28. Dincbas-Renqvist, V., Engstrom, A., Mora, L., Heurgue-Hamard, V., Buckingham, R., and Ehrenberg, M. (2000) A post-translational modification in the GGQ motif of RF2 from *Escherichia coli* stimulates termination of translation. *EMBO J. 19*, 6900–6907.
29. Heurgue-Hamard, V., Champ, S., Mora, L., Merkulova-Rainon, T., Kisselev, L. L., and Buckingham, R. H. (2005) The glutamine residue of the conserved GGQ motif in *Saccharomyces cerevisiae* release factor eRF1 is methylated by the product of the YDR140w gene. *J. Biol. Chem. 280*, 2439–2445.
30. Polevoda, B., Span, L., and Sherman, F. (2006) The yeast translation release factors Mrf1p and Sup45p (eRF1) are methylated, respectively, by the methyltransferases Mtq1p and Mtq2p. *J. Biol. Chem. 281*, 2562–2571.
31. Mora, L., Heurgue-Hamard, V., de Zamaroczy, M., Kervestin, S., and Buckingham, R. H. (2007) Methylation of bacterial release factors RF1 and RF2 is required for normal translation termination in vivo. *J. Biol. Chem. 282*, 35638–35645.
32. Figaro, S., Scrima, N., Buckingham, R. H., and Heurgue-Hamard, V. (2008) HemK2 protein, encoded on human chromosome 21, methylates translation termination factor eRF1. *FEBS Lett. 582*, 2352–2356.
33. Carlsson, J., and Åqvist, J. (2006) Calculations of solute and solvent entropies from molecular dynamics simulations. *Phys. Chem. Chem. Phys. 8*, 5385–5395.
34. Baron, R., and McCammon, J. A. (2008) (Thermo)dynamic role of receptor flexibility, entropy, and motional correlation in protein-ligand binding. *ChemPhysChem 9*, 983–988.
35. Marelius, J., Kolmodin, K., Feierberg, I., and Åqvist, J. (1998) Q: A molecular dynamics program for free energy calculations and empirical valence bond simulations in biomolecular systems. *J. Mol. Graphics Modell. 16*, 213–225, 261.
36. Jorgensen, W. L., Maxwell, D. S., and Tirado-Rives, J. (1996) Development and Testing of the OPLS All-Atom Force Field on Conformational Energetics and Properties of Organic Liquids. *J. Am. Chem. Soc. 118*, 11225–11236.
37. Jorgensen, W. L., Chandrasekhar, J., Madura, J. D., Impey, R. W., and Klein, M. L. (1983) Comparison of simple potential functions for simulating liquid water. *J. Chem. Phys. 79*, 926–935.
38. King, G., and Warshel, A. (1989) A Surface Constrained All-Atom Solvent Model for Effective Simulations of Polar Solutions. *J. Chem. Phys. 91*, 3647–3661.
39. Lee, F. S., and Warshel, A. (1992) A Local Reaction Field Method for Fast Evaluation of Long-Range Electrostatic Interactions in Molecular Simulations. *J. Chem. Phys. 97*, 3100–3107.
40. Ryckaert, J.-P., Ciccotti, G., and Berendsen, H. J. C. (1977) Numerical integration of theCartesian equations of motion of a system with constraints: Molecular dynamics of n-alkanes. *J. Comput. Phys. 23*, 327–341.

BI900117R